International Journal of Microwave and Wireless Technologies

cambridge.org/mrf

A compact band-notched antenna with high isolation for UWB MIMO applications

Issmat Shah Masoodi, Insha Ishteyaq, Khalid Muzaffar and M. Idrees Magray

Department of Electronics and Communication, Islamic University of Science and Technology, Awantipora, J and K, India

Research Paper

Cite this article: Masoodi IS, Ishteyaq I, Muzaffar K, Magray MI (2021). A compact band-notched antenna with high isolation for UWB MIMO applications. *International Journal of Microwave and Wireless Technologies* **13**, 634–640. https://doi.org/10.1017/S1759078720001427

Received: 18 February 2020
Revised: 21 September 2020
Accepted: 22 September 2020
First published online: 20 October 2020

Key words:
Compact; high isolation; monopole; UWB MIMO antennas; WLAN band notch

Author for correspondence:
Issmat Shah Masoodi,
E-mail: Issmat.shah@islamicuniversity.edu.in

Abstract

A compact antenna module with a single band notch at wireless local area network (WLAN) (5.725–5.825 GHz) for ultra-wideband (UWB) multiple input multiple output (MIMO) applications is proposed. Proposed antenna which acquires size of $0.299\ \lambda \times 0.413\ \lambda \times 0.005\ \lambda\ \text{mm}^3$ at 3.1 GHz consists of two symmetrical radiators placed side by side on global merchandise link (GML) 1000 substrate ($\epsilon_r = 3.2$, $\tan\delta = 0.004$). Isolation between the antenna elements is >18 dB in the whole UWB band, which is achieved by introducing the vertical stub and H-slot between the monopole radiators in the ground plane. The simulated and measured results of the antenna system are in good agreement. The proposed antenna covers entire UWB with impedance bandwidth ($|S_{11}| < -15$ dB) from 3.1 to 11 GHz except at WLAN notched band. The designed antenna module bears low envelope correlation coefficient and minimal multiplexing efficiency hence fulfilling criteria suitable for various wireless MIMO applications.

Introduction

Multiple input multiple output (MIMO) and ultra-wideband (UWB) are the key technologies in this era leading to the rapid development of wireless communication systems. MIMO is a technique, which deploys multiple antennas at input and output terminals of wireless communication systems. As a result, signal to noise ratio (SNR) as well as capacity/data rate of the communication system gets enhanced. MIMO also helps in the reduction of multi-path fading thus increasing the performance of the system [1]. The major problem faced in designing the MIMO antenna system is the electromagnetic isolation between various antenna elements taking into consideration the availability of limited space [2].

UWB is a short-range communication technology, which operates in the frequency band (3.1–10.6 GHz). US-FCC (Federal Communications Commission) allocated this frequency band in 2002 and made this band unlicensed. UWB suffers from the chance of interference due to various parasitic narrowband communication systems such as worldwide interoperability for microwave access (WiMAX) (3.3–3.8 GHz) and wireless local area network (WLAN) (2.4–5.85 GHz). Thus, in order to make UWB communication reliable, antennas should possess band-notch characteristics.

The main factors that yield to the efficient designing of UWB MIMO antenna are high impedance bandwidth, less coupling which results in high isolation, low envelope correlation coefficient, and high diversity gain [3]. Till now, various UWB MIMO antennas with band-notched characteristics have been designed to achieve better wideband and isolation characteristics between various antenna elements [4–7]. In [8], band notching is obtained at WiMAX and WLAN frequencies by inserting an open-ended slot on the radiator and an inverted U-shaped slot on the ground plane. Isolation at lower frequencies (3–4.5 GHz) of UWB antenna has been achieved by introducing a narrow slot in the ground plane [9]. In [10], WLAN band-notched UWB MIMO antenna is proposed consisting of two orthogonally placed antenna elements thus achieving 18 dB electromagnetic isolation.

This paper presents a compact WLAN band-notched UWB antenna with an overall size of $29 \times 40 \times 0.508\ \text{mm}^3$ for MIMO applications. The vertical stub in the ground plane is introduced in order to decrease the mutual coupling between antenna elements. The antenna module acquires impedance bandwidth from 3.1 to 11 GHz and isolation/decoupling of more than 18 dB over the entire operating frequency band. Split ring resonator (SRR) is introduced in order to achieve the notched characteristics at WLAN band. Also, the proposed antenna attains very low envelope correlation coefficient (ECC) value of <0.0005 in the whole operating band except at the notched band thereby decreasing loss in multiplexing efficiency.

Two element UWB MIMO antenna design and analysis

All full-wave antenna simulations were done in computer simulation technology Microwave Studio® Software. Proposed antenna module consists of two symmetrical cup-shaped

CAMBRIDGE UNIVERSITY PRESS

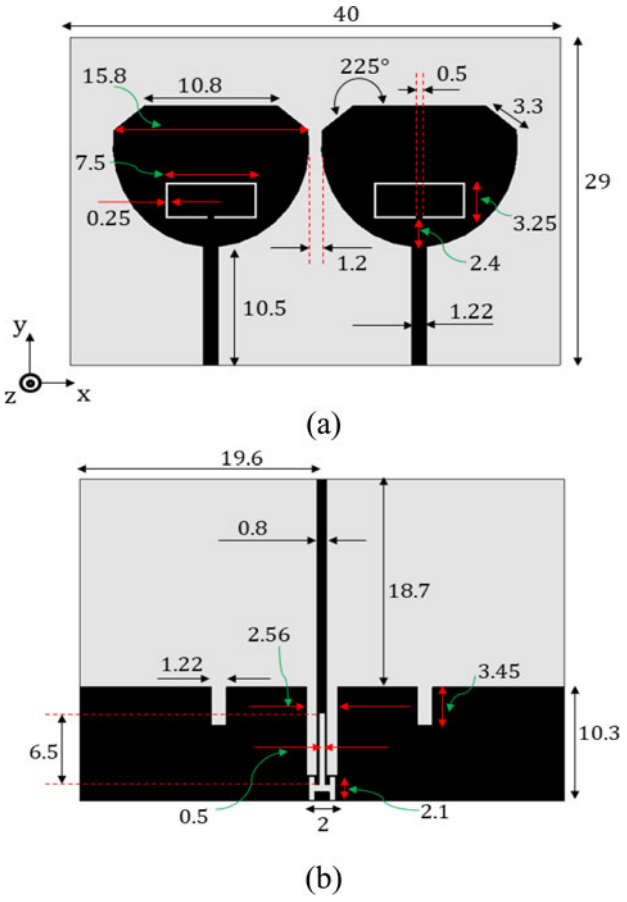

Fig. 1. Schematics of the proposed UWB MIMO antenna: (a) top plane and (b) ground plane (all dimensions are in mm).

monopole radiators placed on global merchandise link (GML) 1000 substrate with the total volume of 0.299 $\lambda \times 0.413\ \lambda \times 0.005\ \lambda\ \text{mm}^3$ at 3.1 GHz. Schematics of the proposed UWB MIMO antenna module is depicted in Figs 1(a) and 1(b) with top and ground planes, respectively.

In the design process of the antenna module, single antenna element with WLAN band notch is designed first. Single element antenna consists of cup-shaped radiator excited with 50 Ω characteristic impedance feed line. The radiator is truncated along the edges to increase the current path and therefore achieving wider impedance bandwidth. The next step in the design process is the placement of another identical antenna element at some distance in mirror configuration about the *y*-axis. The distance between the radiators is adjusted till the isolation/decoupling is <−15 dB and the distance at which it is attained is 1.18 mm (0.012 λ at 3.1 GHz). Vertical stub in the common ground plane is introduced so as to achieve better isolation. Moreover, to enhance the isolation between the monopole radiators, slots are etched out in the ground plane. Also, the radiating monopoles are truncated from the top side so as to increase the impedance matching and isolation at a higher frequency band (6–8 GHz). The fabricated prototype of the proposed UWB MIMO antenna module with front and back views is shown in Fig. 2.

For impedance matching, the rectangular slots under the respective feed lines of two ports in the shared ground plane are etched out. The slots produce a capacitive effect which nullifies inductive effect created by the structure topology, thence

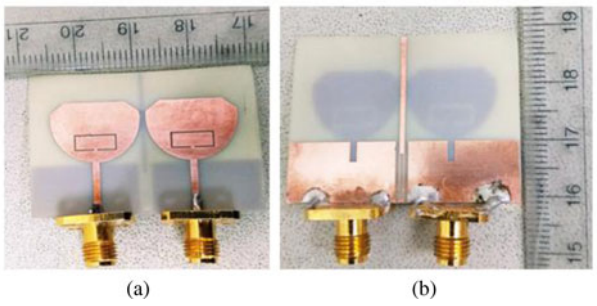

Fig. 2. Fabricated photograph of the proposed prototype: (a) top plane and (b) ground plane.

improving impedance matching. Vertical ground stub acting as a monopole is inserted between the radiators to improve isolation/decoupling. The length of the stub determines the frequency at which resonance will occur. As seen from Fig. 1, the total length of vertical stub is 26.7 mm (0.55 $\lambda_{\text{at3.1 GHz}}/2$) and it is controlled by the length of the slot which is etched out next to the vertical stub. The ground surface currents get distributed along this vertical stub, thus increasing path of the current and hence increasing the isolation between monopole radiators. An H-shaped slot in the ground plane is also cut in order to enhance the impedance matching and isolation in the frequency band (6.5–7.5 GHz). The length of H-slot is around $\lambda/4$ at 7 GHz which resonates thereby concentrating ground surface currents along it and therefore leading to isolation and impedance matching improvement. Figure 3 shows the effect of H-slot on S-parameters and isolation.

SRR is introduced in both of the antenna elements as shown in Fig. 1 in order to filter out the undesired/parasitic frequencies. The notched characteristics are obtained at WLAN band (5.725–5.825 GHz). The input impedance of antenna becomes high at notched frequency band behaving like an open-circuit thereby rejecting frequencies in the WLAN band. Return Loss and Isolation of the proposed antenna without SRR is shown in Fig. 4.

The total average length of the SRR is $\lambda/2$ at the desired frequency and is calculated by [3]:

$$L_r = \frac{c}{2f\sqrt{\varepsilon_{eff}}}, \tag{1}$$

where

$$\varepsilon_{eff} = \frac{\varepsilon_r + 1}{2}, \tag{2}$$

is the effective dielectric constant and "*c*" is the speed of light.

Results and discussions

Measured results of the proposed antenna were carried out using Agilent PNA E8364C. Simulated and measured Return Loss ($-20\log|S11|$) of the fabricated antenna is shown in Fig. 5. It can be seen that the proposed antenna covers the whole UWB with WLAN Band (5.725–5.825 GHz) notched characteristics. Also, the simulated result shows that the operating bands of the antenna range from 3.3 to 5.5 GHz and 5.85–11 GHz. Moreover, simulated as well as measured isolation is almost <−20 dB in the whole UWB.

https://doi.org/10.1017/S1759078720001427 Published online by Cambridge University Press

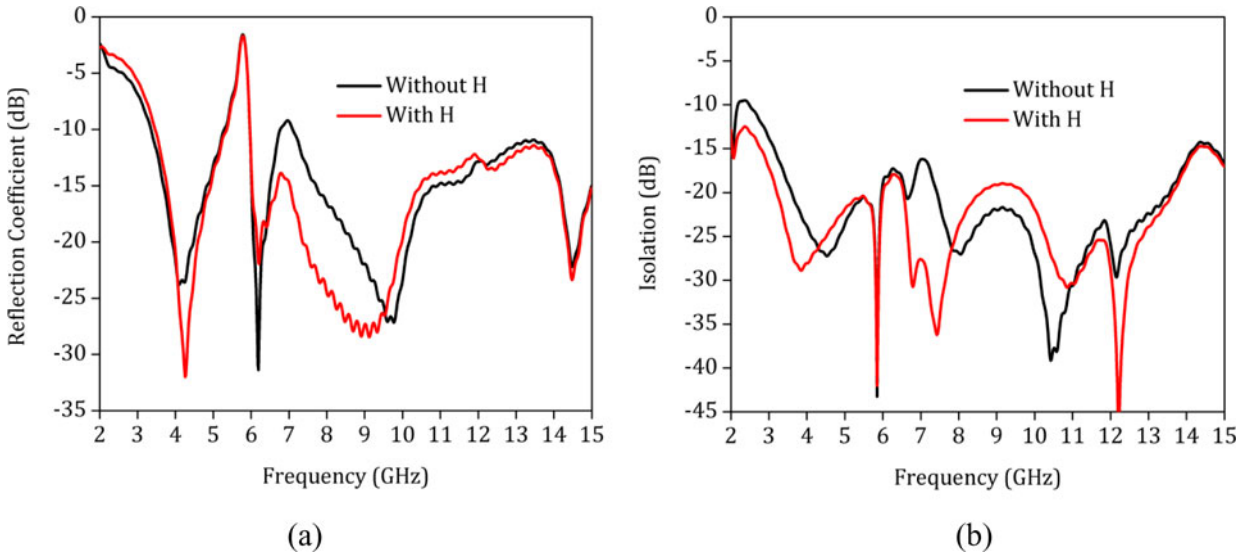

Fig. 3. Effect of H-slot on (a) return loss and (b) mutual coupling.

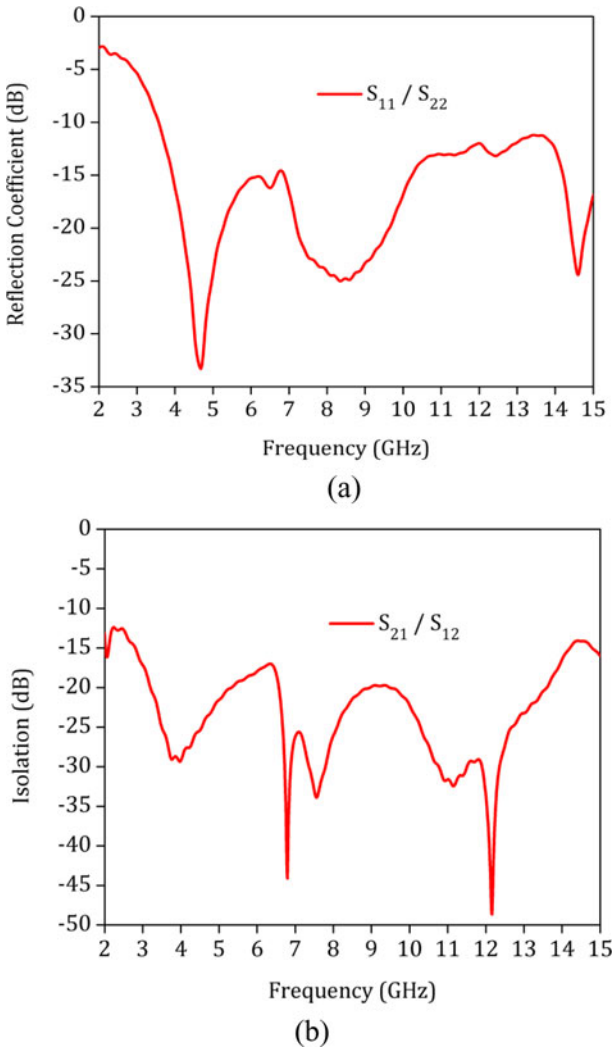

Fig. 4. Effect of SRR on (a) return loss and (b) mutual coupling.

Discrepancies between simulated and measured S-parameters might be due to the following reasons:

1. Relative permittivity of the fabricated prototype might be inhomogeneous compared to assumed relative permittivity of substrate used in the simulation. The dielectric constant exhibits some frequency dependency and a corresponding frequency shift is illustrated in Fig. 6.
2. The connector and coax to antenna transition might be offering frequency sensitive lead inductance leading to a higher discrepancy.
3. The coax to microstrip transition assumed in the simulations and the actual fabricated prototype is quite different, due to the nature of SMA connector itself. The SMA connector assumed in simulations has a round pin while the practical SMA connector has a flat pin transitioning to the microstrip which would produce quite different results especially at higher frequencies.
4. Lack of frequency sensitive calibration of the VNA including the cables and connectors/adapters.
5. Soldering of SMA connector at high temperatures is hard due to brittle nature of GML 1000 substrate which might lead to discontinuities between the microstrip feed line and SMA connector.
6. Fabrication tolerances can also cause a disparity between simulation and measured data.

Furthermore, the current distribution at 4, 5.75, and 7 GHz are shown in Fig. 7. At a lower frequency of 4 GHz when the UWB MIMO antenna is fed through Port 1, the current gets distributed along the vertical stub and H-slot which increases the path of surface current thus resulting in better isolation between the antenna elements. At 5.75 GHz, the entire surface current gets distributed along the SRR thus filtering out the desired frequency as can be seen in Fig. 7(b). At 7 GHz, the surface current gets coupled through vertical stub and H-slot which increases the electromagnetic isolation between monopole radiators thus reducing ECC.

https://doi.org/10.1017/S1759078720001427 Published online by Cambridge University Press

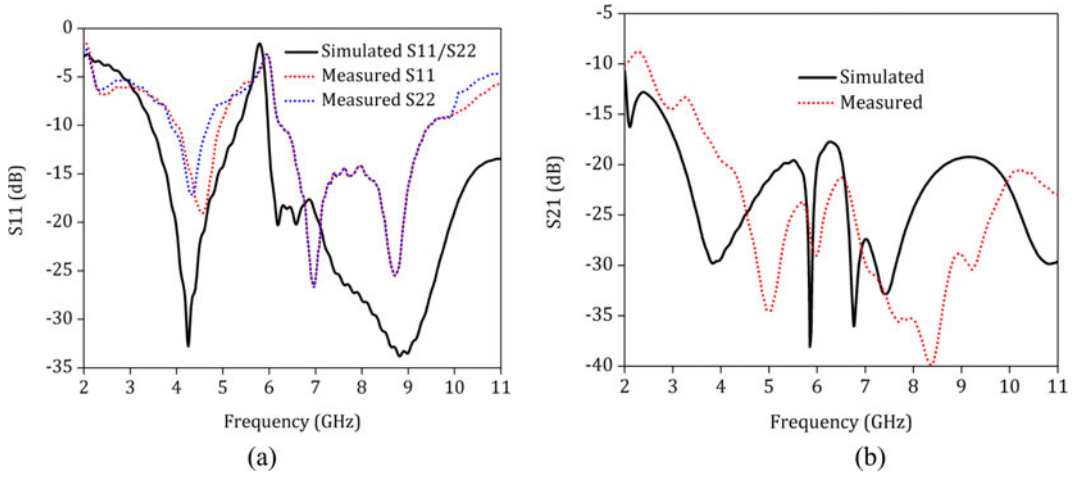

Fig. 5. Simulated and measured (a) S_{11}/S_{22} and (b) S_{21} of the proposed UWB MIMO antenna.

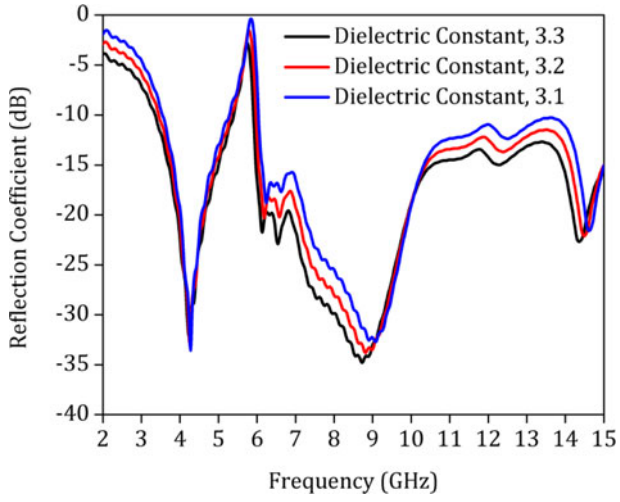

Fig. 6. Frequency dependency of dielectric constant (ϵ_r) of the proposed UWB antenna.

Performance characteristics of proposed single-band notched UWB MIMO antenna

Radiation pattern performance

Simulated and measured co-pol and cross-pol radiation patterns of the proposed antenna at frequencies 4, 7 and 10 GHz are illustrated in Fig. 8. Measured radiation patterns were obtained inside an anechoic chamber by placing the far-field system set-up for various radiation pattern measurements. Measurement is performed by exciting one of the ports (Port 1 or Port 2) while the other remaining port is terminated with 50Ω matched load. Simulated and measured radiation patterns are plotted for both ports, Port 1 and Port 2 in the *XOZ* plane. As can be seen from Fig. 8, the measured radiation patterns follow the simulated patterns and are stable in the whole UWB. Discrepancies might be due to some reflections produced from radiation-absorbent material of the anechoic chamber. Radiation patterns are almost Omni-directional in the given set of frequencies indicating the monopole behavior of the proposed antenna. Cross-polarization of the proposed antenna is <10 dB which is reasonably high due to usage of the thick substrate. In addition to this, the polarization impurity of the proposed UWB antenna can also increase cross-polarization.

Gain and radiation efficiency

Gain and radiation efficiency of the proposed antenna is depicted in Fig. 9. Gain is measured by gain transfer method in an anechoic chamber using standard Keysight horn antennas [11]. Gain varies from 2 to 4.9 dBi over the entire operating band except at notched frequencies where gain drops to negative. As UWB technology is meant for short-range communication, therefore gain is reasonably good. Moreover, the radiation efficiency is high at operating frequencies varying between 80 and 92% which is primarily due to low dielectric loss tangent of the substrate and low value of input reflection coefficient. Simulated radiation efficiency varies across the whole operating band which may be due to the frequency dependency of the dissipation factor of substrate. Since, both the antenna elements are identical and symmetrical about *Y*-axis with same return loss characteristics, gain and radiation efficiency plots, therefore, remain invariant.

ECC performance characterization

ECC is the important factor regarding the performance characterization of MIMO antenna. To avoid the inaccuracies in calculating ECC from S-parameters, ECC is rather calculated from the expressions which are based on far-field radiation patterns as given in [12]. Since the calculation of S-parameters is only applicable to the currents flowing at the physical ports, therefore cross-correlation evaluation cannot be reduced to the calculation of S-parameters as the former depends upon entire current on the antenna surfaces. Thus, ECC calculated from far-field radiation patterns is shown below:

$$\rho = \frac{\left|\int_{4\pi} d\Omega\ \mathbf{E}_1\ (\theta, \phi)\ \ \mathbf{E}_2^*\ (\theta, \phi)\ \right|}{\sqrt{\int_{4\pi} d\Omega\ |\mathbf{E}_1\ (\theta, \phi)|^2}\ \sqrt{\int_{4\pi} |\mathbf{E}_2\ (\theta, \phi)|^2}}, \tag{3}$$

where $\mathbf{E}_1\ (\theta, \phi)$ and $\mathbf{E}_2\ (\theta, \phi)$ are radiation patterns of antenna elements 1 and 2 respectively, Ω is the solid angle and "*" denotes the complex conjugate operator. As shown in Fig. 10(a), ECC

https://doi.org/10.1017/S1759078720001427 Published online by Cambridge University Press

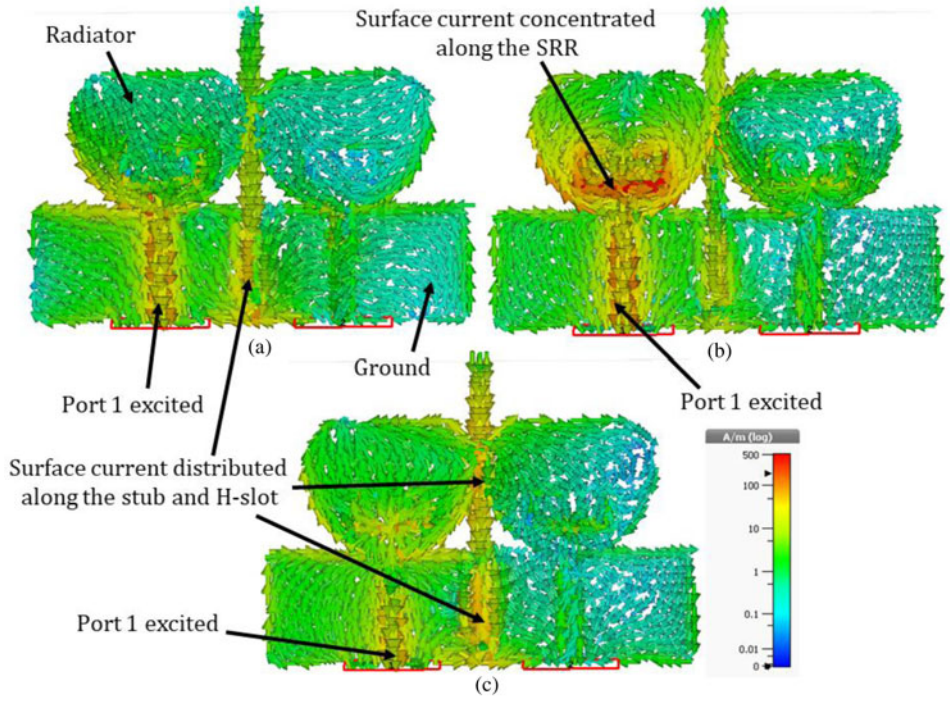

Fig. 7. Surface current distribution of proposed antenna module at (a) 4 GHz, (b) 5.75 GHz, and (c) 7 GHz.

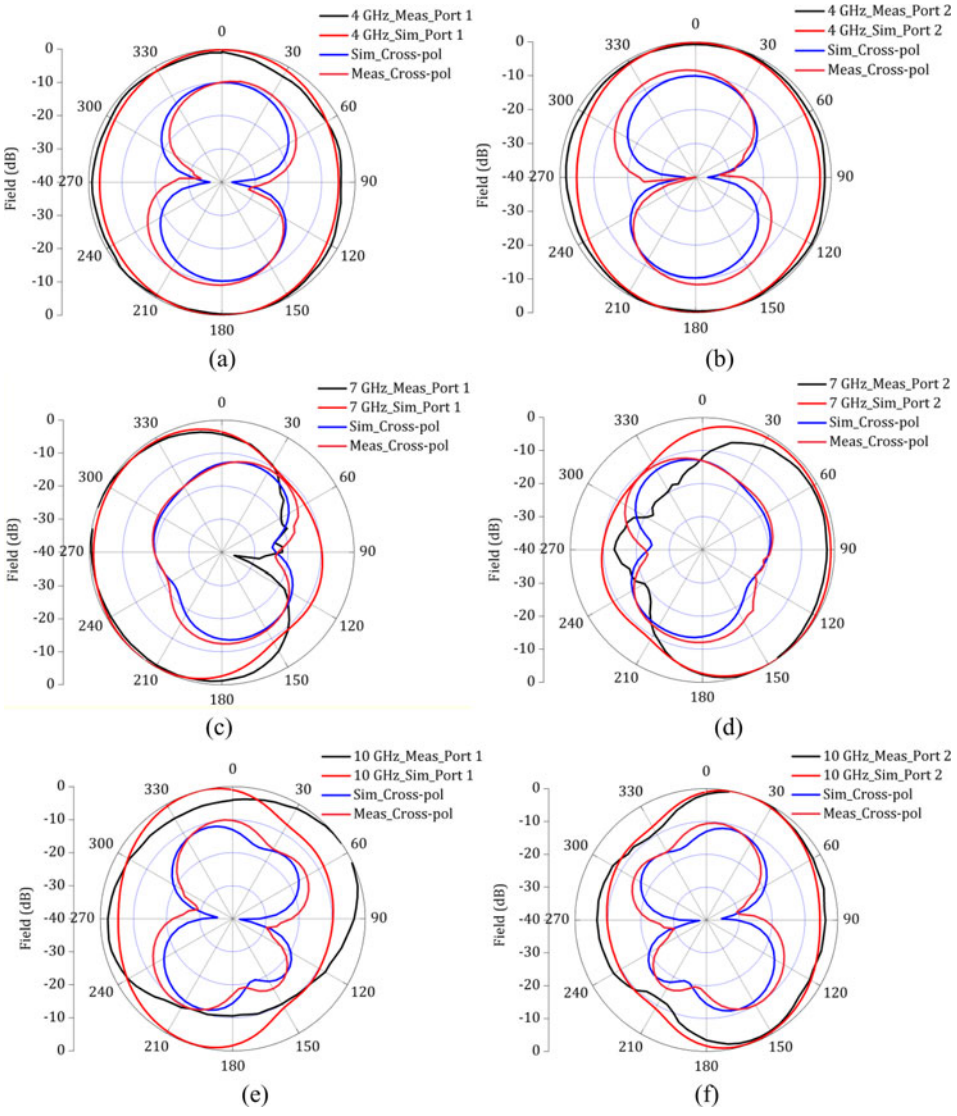

Fig. 8. Simulated and measured radiation patterns of the proposed antenna in *XOZ*-plane at 4, 7, and 10 GHz for both the antenna elements.

https://doi.org/10.1017/S1759078720001427 Published online by Cambridge University Press

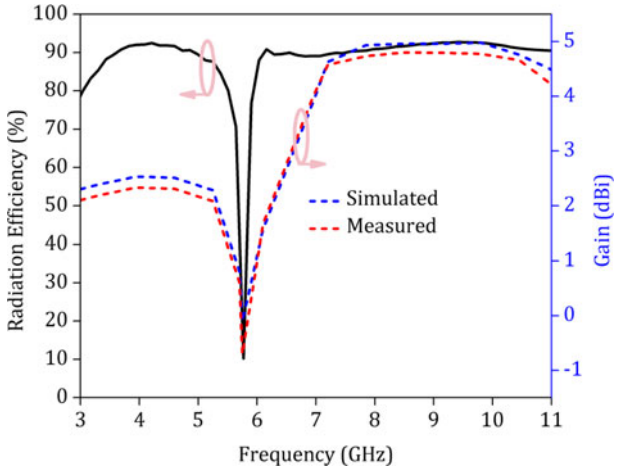

Fig. 9. Gain and radiation efficiency plots of the proposed WLAN band-notched UWB antenna.

takes values below 0.0005 except at the frequency band where notch occurs. This low value of ECC proves that the proposed UWB MIMO antenna is best for diversity applications.

Multiplexing characterization

The multiplexing efficiency η_{mux} is defined as the loss in power efficiency which occurs while using MIMO antenna-under-test to achieve the same channel capacity as that of an ideal MIMO antenna system [13]. The value of multiplexing efficiency should be very minimum. As can be realized from Fig. 10(b), (η_{mux}) η_{mux} takes values <−0.5 dB in the entire UWB, except at the notched frequency band.

Comparison between proposed single band-notched UWB MIMO antenna and recently reported UWB MIMO antennas is illustrated in Table 1.

Conclusion

Two element UWB MIMO antenna module with WLAN band notch characteristics is proposed. Vertical stub and H-slot is introduced between the monopole antennas in order to increase isolation (>18 dB). Performance parameters like radiation pattern, ECC, and multiplexing efficiency are included with technical

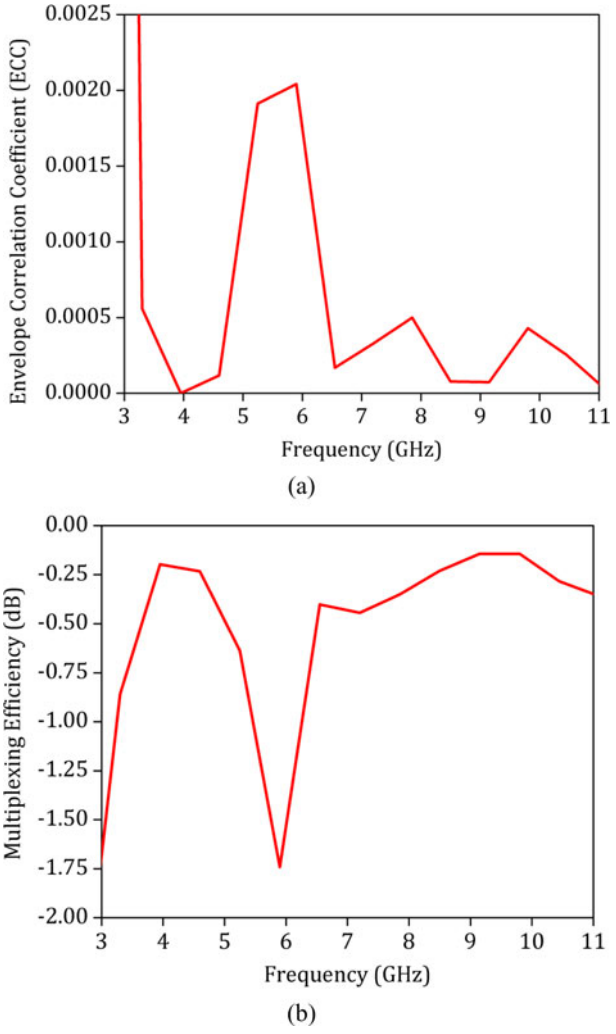

Fig. 10. Simulated (a) ECC and (b) multiplexing efficiency of the proposed antenna module.

Table 1. Comparison of proposed single band-notched UWB MIMO antenna with other recently reported designs.

Reference	Volume of antenna module (mm^3)	Minimum isolation (dB)	Peak Gain (dBi)	Envelope correlation coefficient	Multiplexing efficiency (dB)
This work	589.28	−18	2–4.9	<0.0005	<−0.5
[3]	840	−20	2.4–5	<0.015	Not available
[4]	995.4	−20	2–5.2	<0.03	Not available
[5]	780	−20	2–5.2	<0.01	Not available
[6]	1036.8	−20	1.6–6	<0.012	<−1.2
[7]	2240	−16	Not available	<0.0003	Not available
[14]	582.4	−15	1.6–4	<0.08	<−4
[15]	665.6	−18	0.7–6.86	<0.08	Not available
[16]	1036.8	−20	−4–4	<0.05	<−1
[17]	716.8	−20	1.2–6.8	<0.04	Not available
[18]	436.8	−15	1.6–6.2	<0.02	Not available

https://doi.org/10.1017/S1759078720001427 Published online by Cambridge University Press

justifications. These parameters lie within desired limits in the whole UWB making this antenna suitable for UWB MIMO antenna systems.

Acknowledgement. The authors would like to thank the Centre for Applied Research in Electronics (CARE) department of IIT Delhi for providing antenna testing facility.

References

1. **Foschini GJ and Gans MJ** (1998) On limits of wireless communications in a fading environment when using multiple antennas. *Wireless Personal Communication*, **6**, 311–335.
2. **Tang Z, Wu X, Zhan J, Hu S, Xi Z and Liu Y** (2019) Compact UWB-MIMO antenna with high isolation and triple band-notched characteristics. *IEEE Access*, **7**, 19856–19865.
3. **Zamir W and Dinesh K** (2015) Dual-band-notched antenna for UWB MIMO applications. *International Journal of Microwave and Wireless Technologies*, **9**, 381–386.
4. **Yadav D, Abegaonkar MP, Koul SK, Tiwari VN and Bhatnagar D** (2018) Two element band-notched UWB MIMO antenna with high and uniform isolation. *Progress In Electromagnetics Reasearch*, **63**, 119–229.
5. **Tang Z, Zhan J, Wu X, Xi Z, Chen L and Hu S** (2020) Design of a compact UWB-MIMO antenna with high isolation and dual band-notched characteristics. *Journal of Electromagnetic Waves and Applications*, **34**, 500–513.
6. **Chandel R and Gautam AK** (2016) Compact MIMO/diversity slot antenna for UWB applications with band-notched characteristic. *Electronics Letters*, **52**, 336–338.
7. **Ibrahim AA and Machacand Shubair JRM** (2017) Compact UWB MIMO antenna with pattern diversity and band rejection characteristics. *Microwave and Optical Technology Letters*, **59**, 1460–1464.
8. **Han L, Chen J and Zhang W** (2020) Compact UWB monopole antenna with reconfigurable band-notch characteristics. *International Journal of Microwave and Wireless Technologies*, **12**, 252–258.
9. **Ren J, Hu W, Yin Y and Fan R** (2014) Compact printed MIMO antenna for UWB applications. *IEEE Antennas Wireless Propagation Letters*, **13**, 1517–1520.
10. **Zhao JY, Zhang ZY, Liu QQ, Fu G and Gong SX** (2014) Printed UWB MIMO antenna with different polarizations and band-notch characteristics. *Progress In Electromagnetics Research Letters*, **46**, 113–118.
11. **Alhalabi RA and Rebeiz GM** (2010) Differentially-fed millimeter-wave Yagi-Uda antennas with folded dipole feed. *IEEE Transactions on Antennas Propagation*, **58**, 966–969.
12. **Mikki SM and Antar YMM** (2015) On cross correlation in antenna arrays with applications to spatial diversity and MIMO systems. *IEEE Transactions on Antennas Propagation*, **63**, 1798–1810.
13. **Tian R, Lau BK and Ying Z** (2012) Multiplexing efficiency of MIMO antennas with user effects. *IEEE International Symposium on Antennas and Propagation (AP-S)*, in press.
14. **Zhao Y, Zhang F-S, Cao L-X and Li D-H** (2019) A compact dual band-notched MIMO diversity antenna for UWB wireless applications. *Progress In Electromagnetics Research C*, **89**, 161–169.
15. **Addepalli T and Anitha VR** (2020) A very compact and closely spaced circular shaped UWB MIMO antenna with improved isolation. *AEU - International Journal of Electronics and Communications* **114**, 153016–153038.
16. **Khan MI and Khattak MI** (2020) Designing and analyzing a modern MIMO-UWB antenna with a novel stub for stop band characteristics and reduced mutual coupling. *Microwave and Optical Technology Letters* **62**(10), 3209–3214.
17. **Addepalli T and Anitha VR** (2020) Compact two-port MIMO antenna with high isolation using parasitic reflectors for UWB, X and Ku band applications. *Progress In Electromagnetics Research C*, **102**, 63–77.
18. **Li D-H, Zhang F-S, Cao L-X and Zhao Y** (2019) A compact dual band-rejected MIMO vivaldi antenna for UWB wireless applications. *Progress In Electromagnetics Research Letters*, **86**, 97–105.

Issmat Shah Masoodi (Graduate Student Member, IEEE) received B.Tech. in Electronics and Communication Engineering from the University of Jammu in 2013 and received his M. Tech from SMVDU, Katra in 2015. Currently, he is pursuing Ph.D. in Electronics and Communication Engineering with Islamic University of Science and Technology (IUST), Awantipora, J and K, India. He has worked as Assistant Professor at University of Kashmir from 2015 to 2018. He has authored/co-authored several articles in peer-reviewed journals and conference proceedings. His main research interests are design of 4G/5G antennas for Smartphones, mmWave antennas for 5G applications and meta-materials.

Insha Ishteyaq (Graduate Student Member, IEEE) received her bachelor's in Electronics and Communication Engineering in 2013 from the University of Kashmir and her masters in 2017. She is currently working towards her Ph.D. degree at the Islamic University of Science and Technology with research interests in antenna design for 5G standards. She has published a few papers in international journals and conferences. Her research interests include modern-day antenna design, millimeter-wave antennas, microelectronics, and related applications.

Khalid Muzaffar (Member, IEEE) received B. Tech in Electronics and Communication Engineering and M. Tech in Communication and IT from NIT Srinagar, India in 2004 and 2006 respectively, and Ph.D. from the Centre for Applied Research in Electronics (CARE) IIT Delhi, India in June 2017. He worked as Field and Maintenance Engineer in Ericsson India Pvt. Ltd. from July 2006 to July 2007. He joined IUST Awantipora, as an Assistant Professor in August 2007. He is currently working as HoD Electronics & Communication Engineering and AICTE coordinator in IUST, Awantipora. His research interests are microwave antenna design, Millimeter-wave MIMO antenna design, High impedance surfaces and applications of thermal imaging for microwave field imaging.

M. Idrees Magray (Graduate Student Member, IEEE) received the B.Tech. degree in electronics and communication engineering from the Islamic University of Science and Technology (IUST), Awantipora, in 2018. He is currently pursuing a master's degree with National Chiao Tung University (NCTU), Taiwan. He received INAE fellowship for 2 months and during that tenure, he worked under the supervision of Professor S. K. Koul. He worked on various projects at CARE, IIT Delhi, under the guidance of Professor S. K. Koul. He has authored or coauthored several articles in peer-reviewed journals and conference proceedings. His research interests include co-designed 4G/5G antennas for smartphones, mmWave antennas for mobile terminals and base stations, and antenna in the packaging (AiP). He received the Best Project Competition Award in InCAP 2019.

https://doi.org/10.1017/S1759078720001427 Published online by Cambridge University Press